Supplemental Figure 1

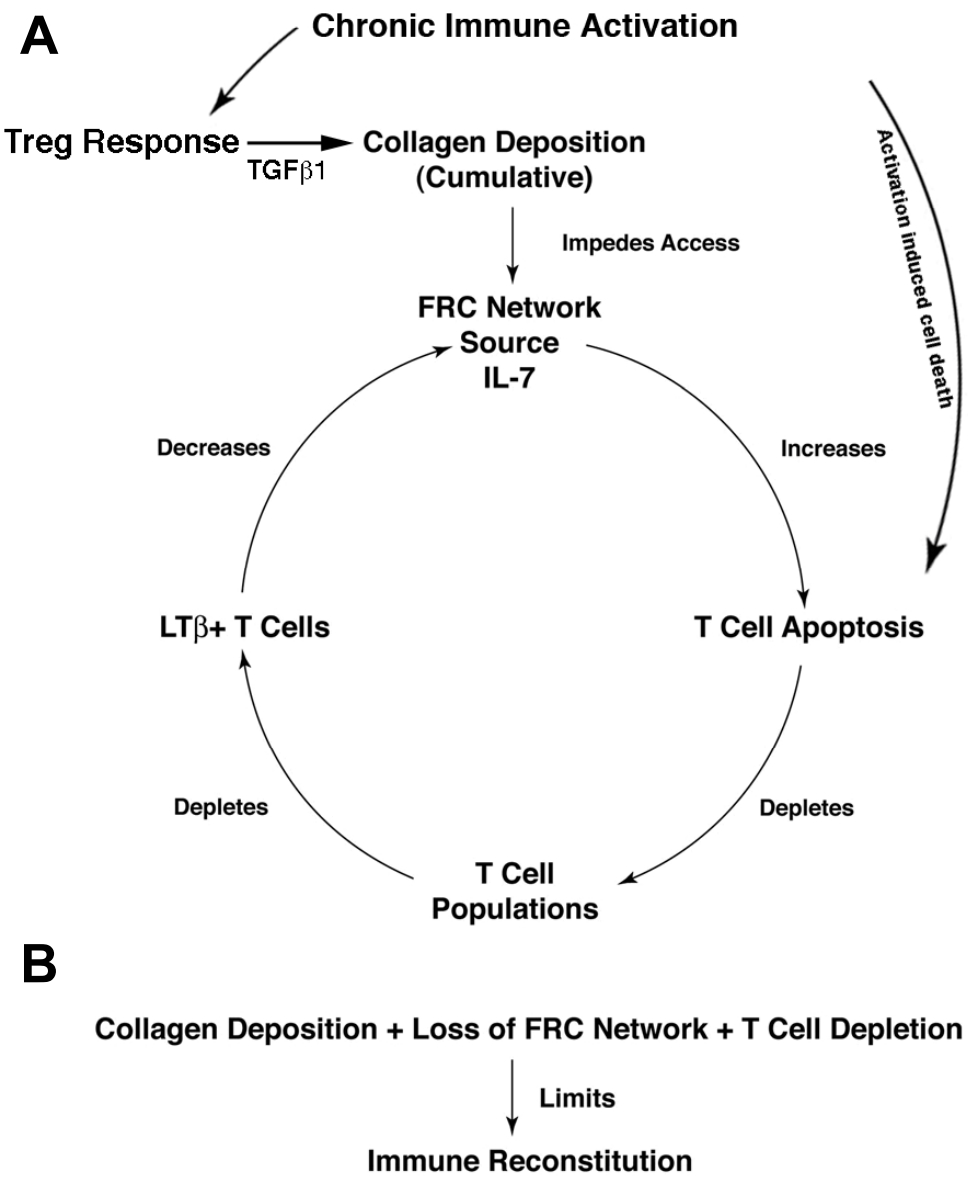

Supplemental Figure 2

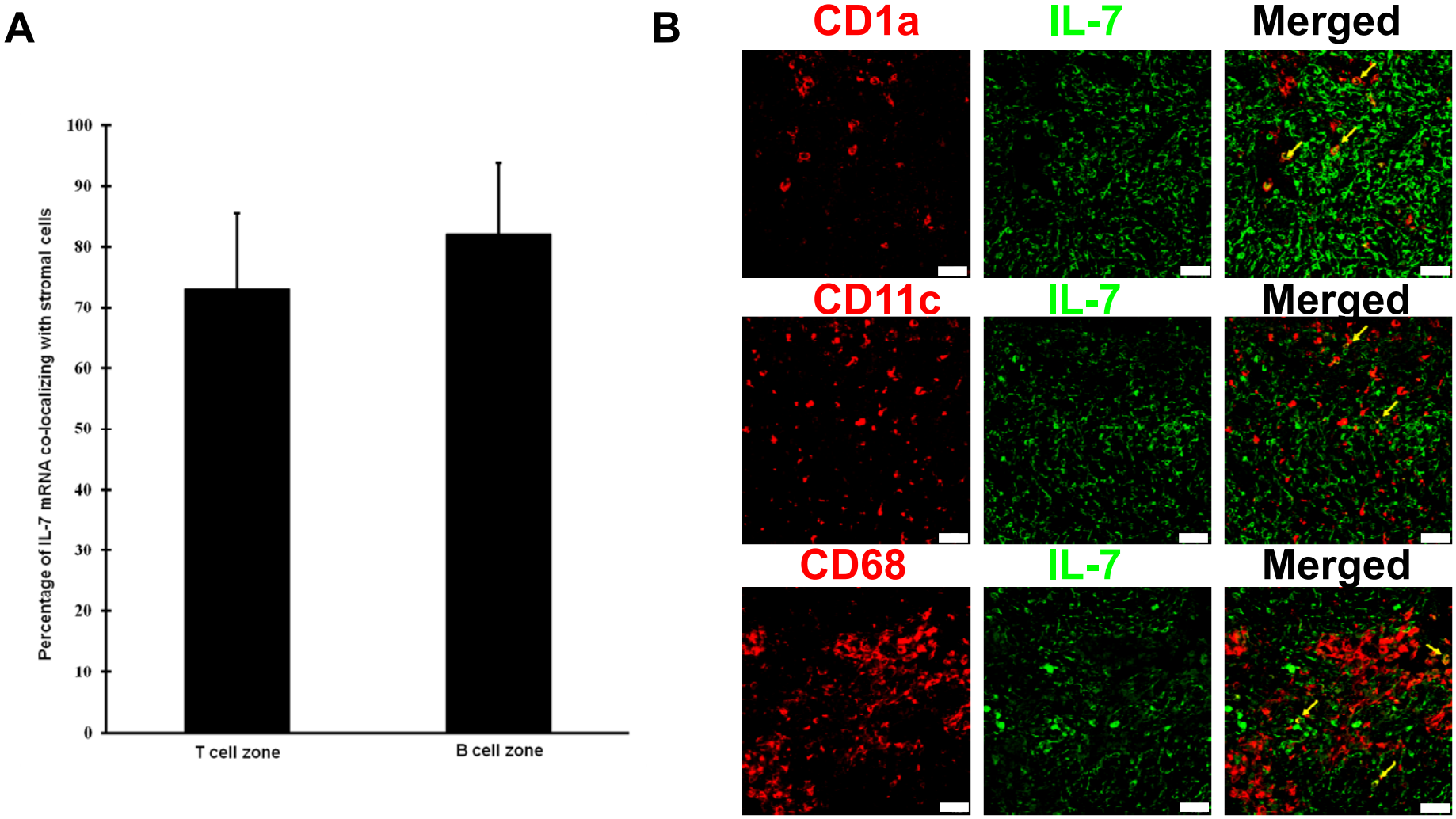

Supplemental Figure 3

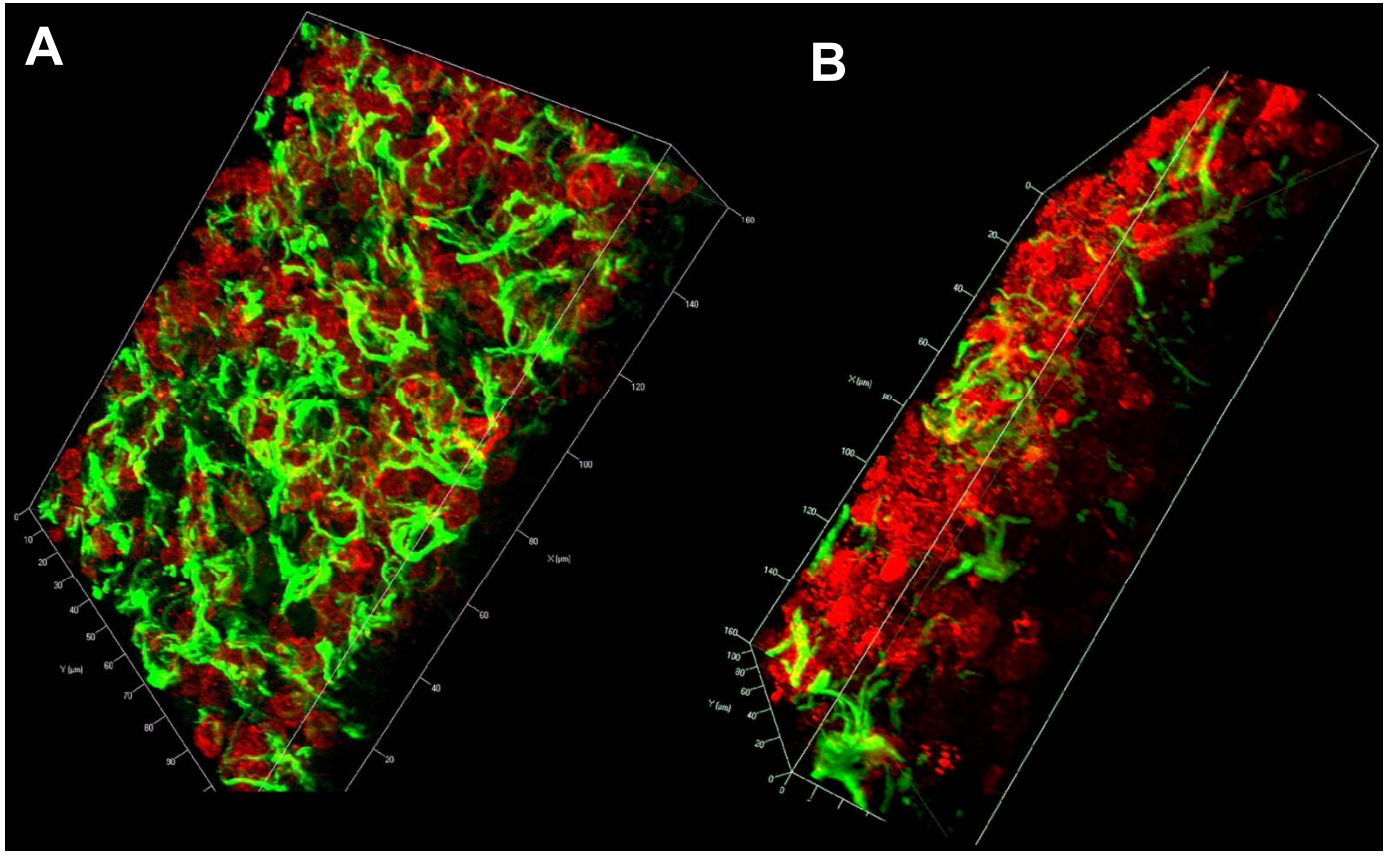

Supplemental Figure 4

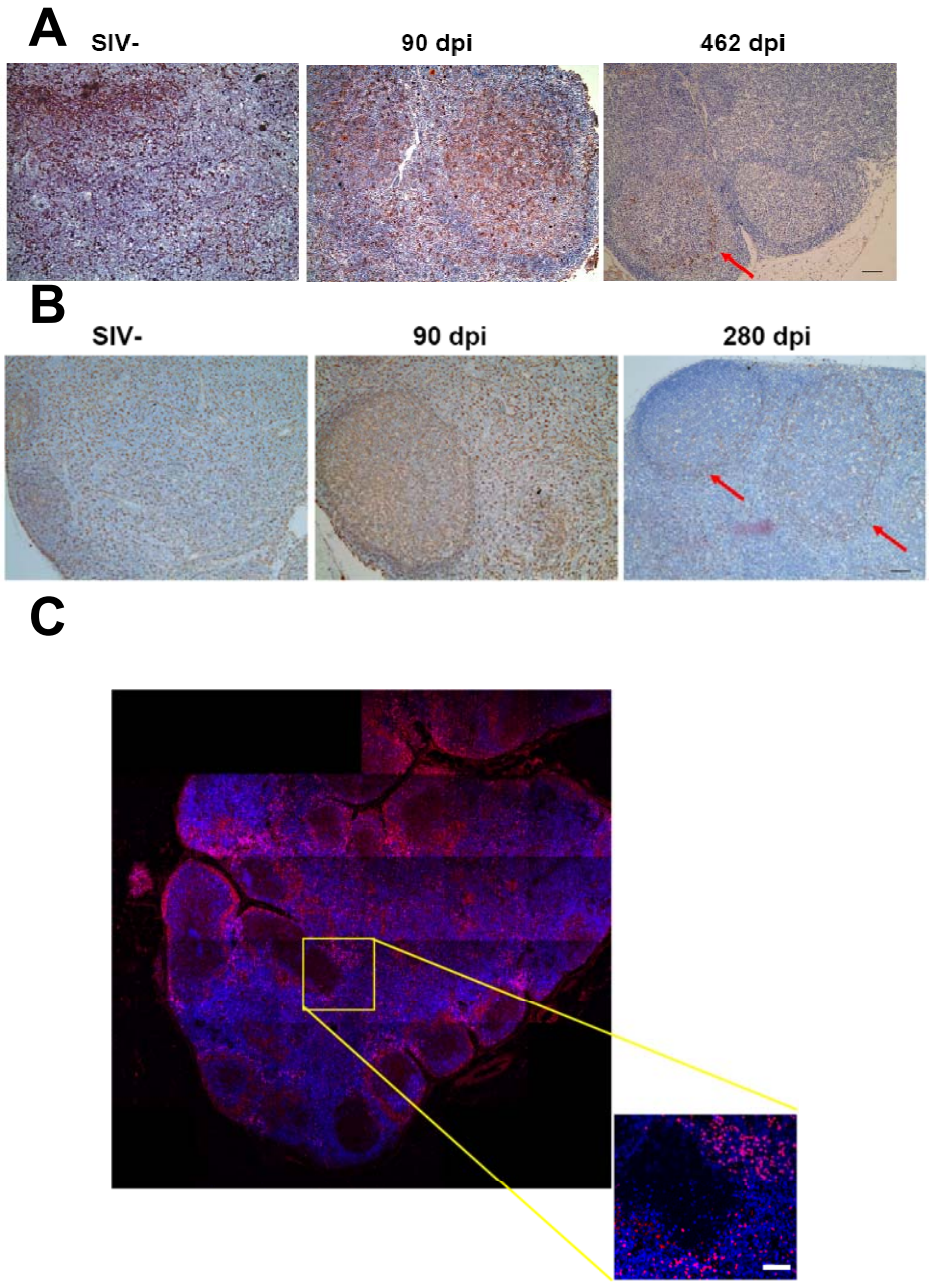

Supplemental Figure 5

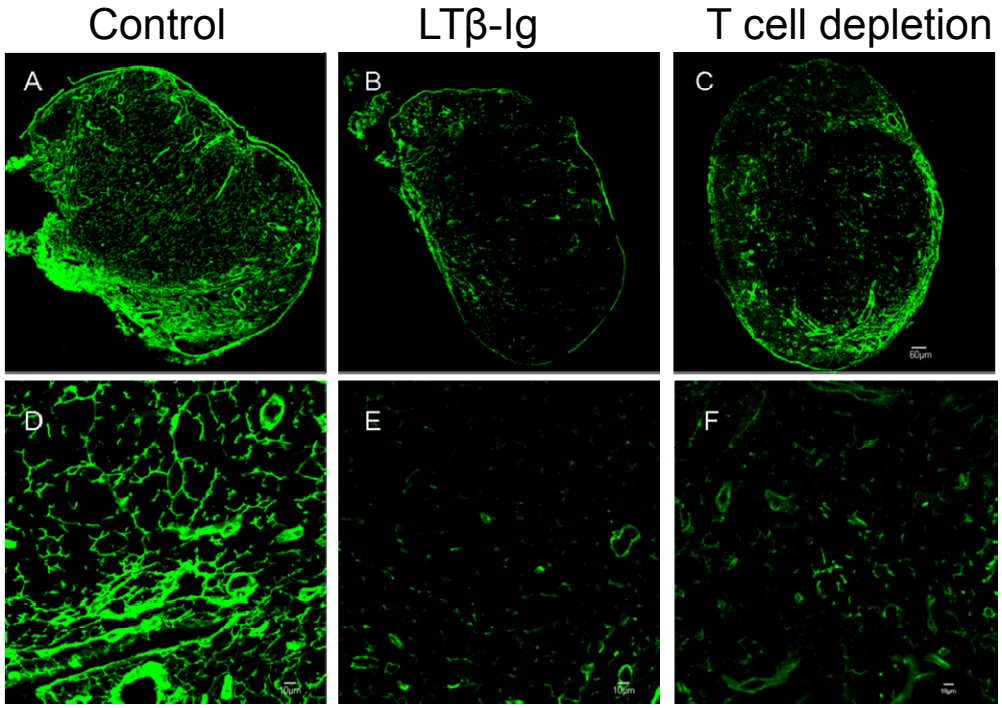

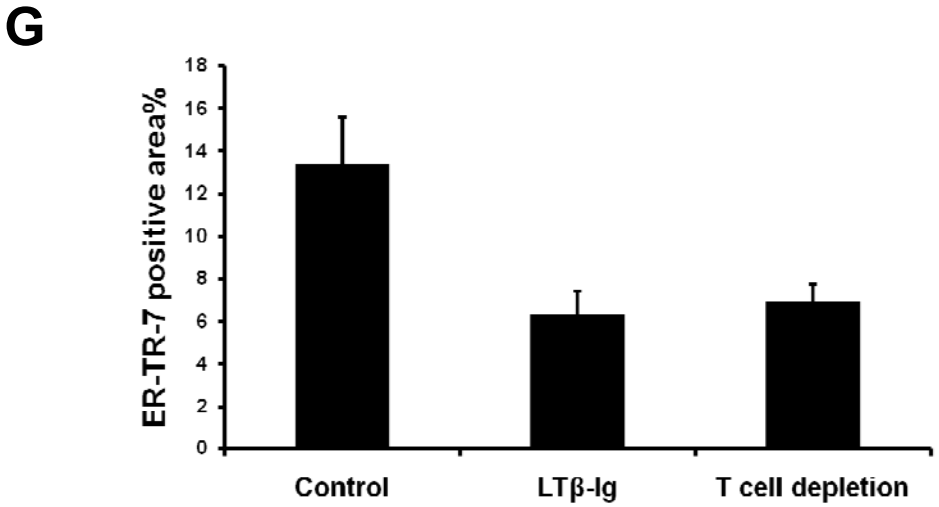

Supplemental Figure 6

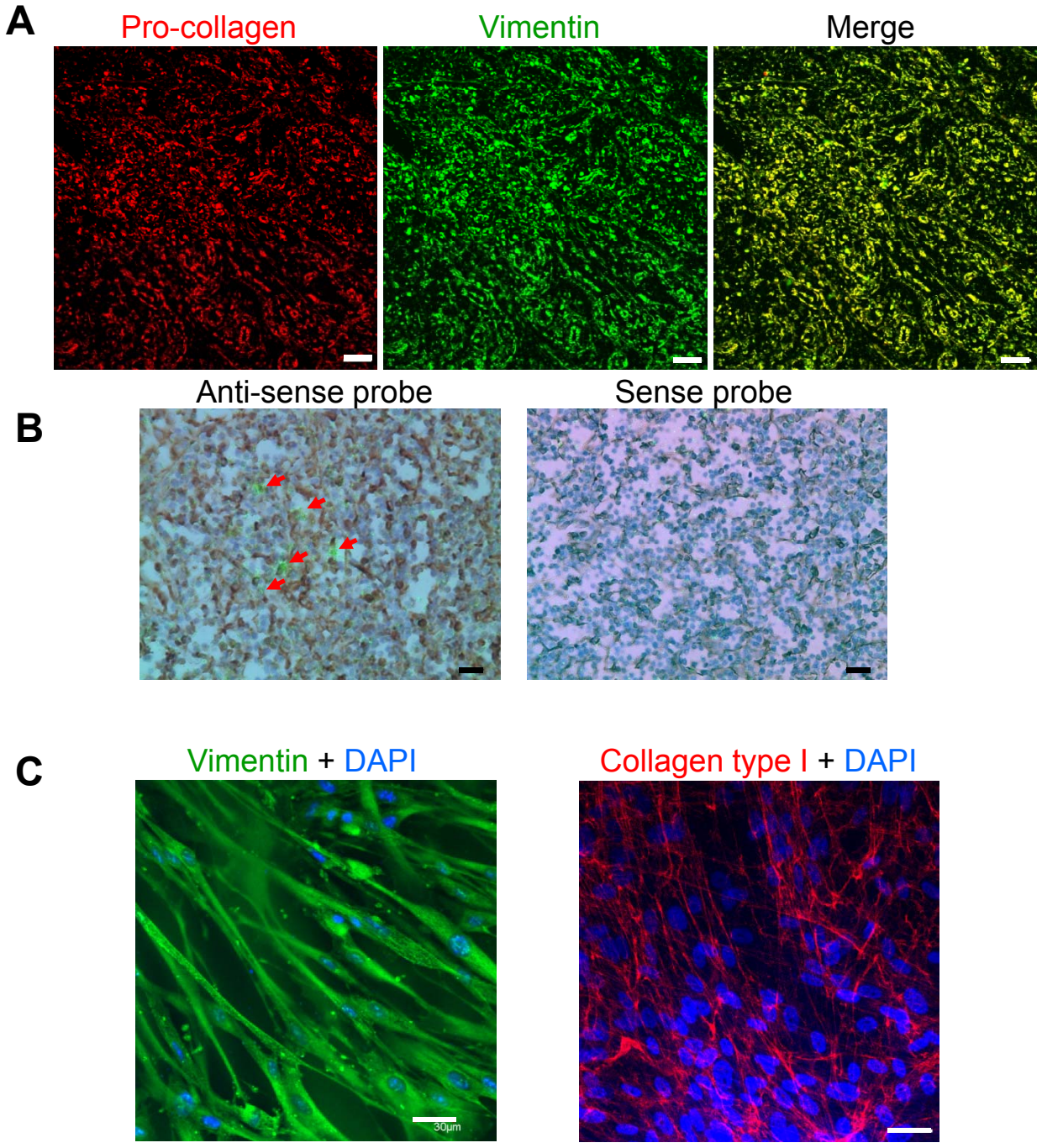

Supplemental Figure 7

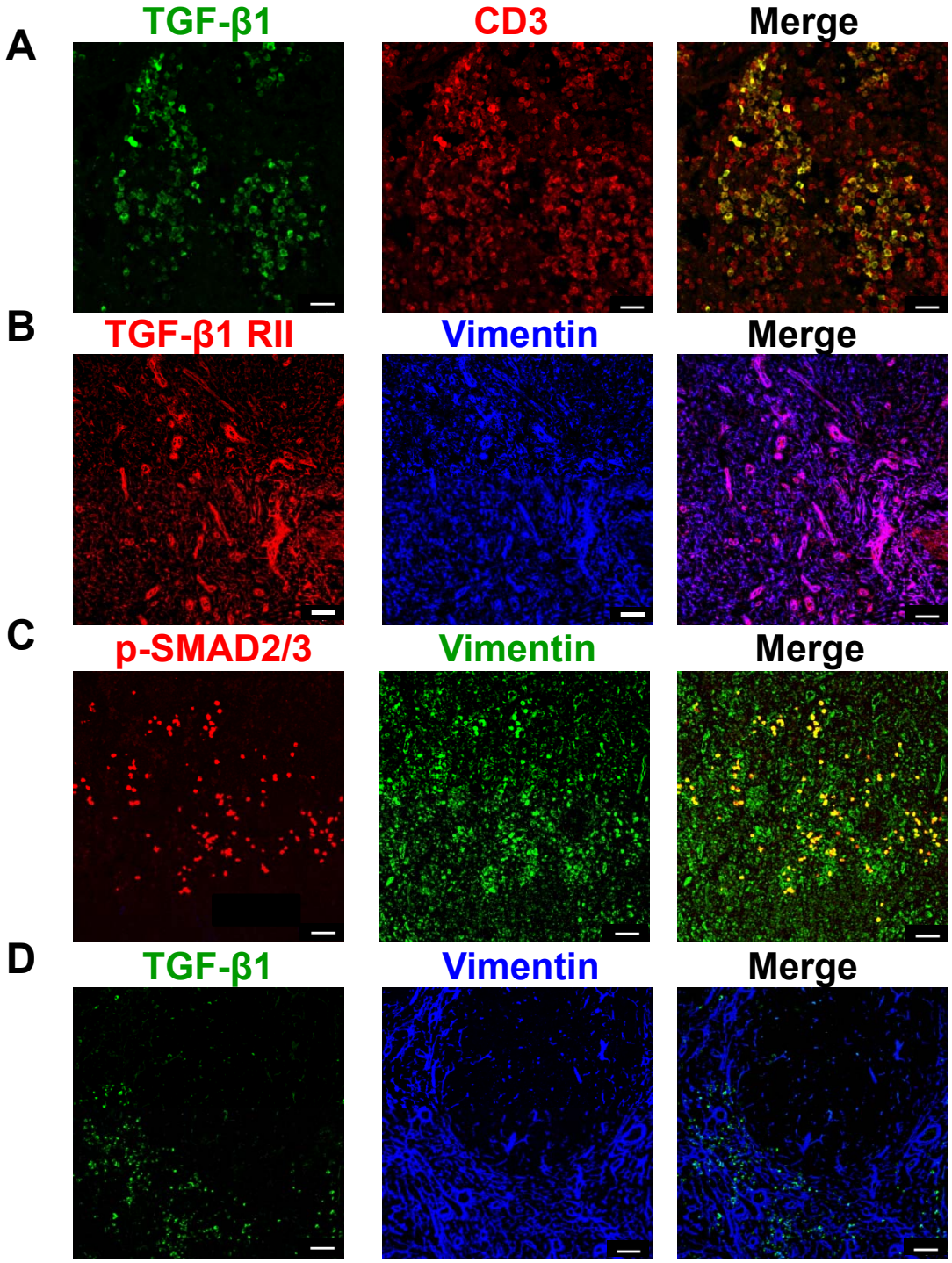

Supplemental Figure 8

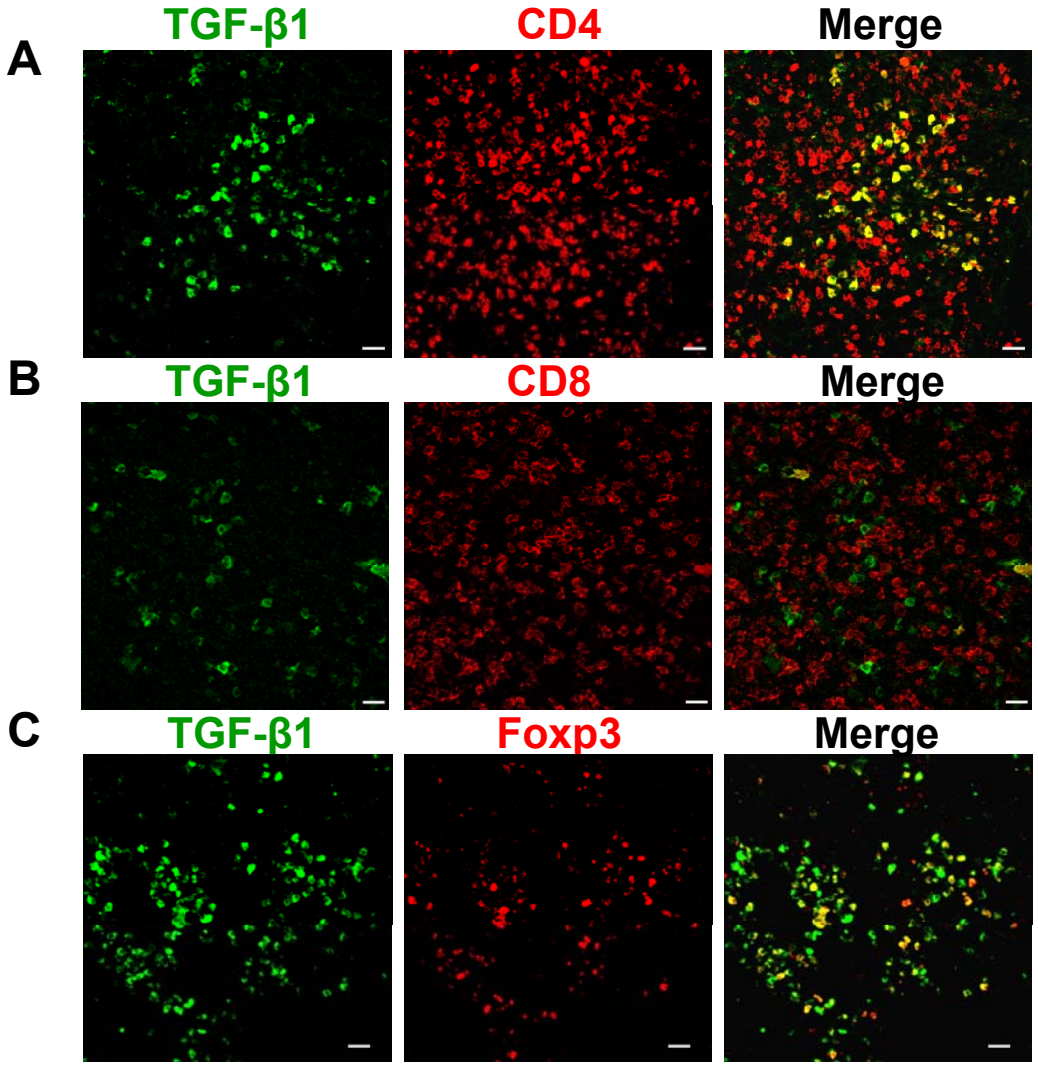

Supplemental Figure 9

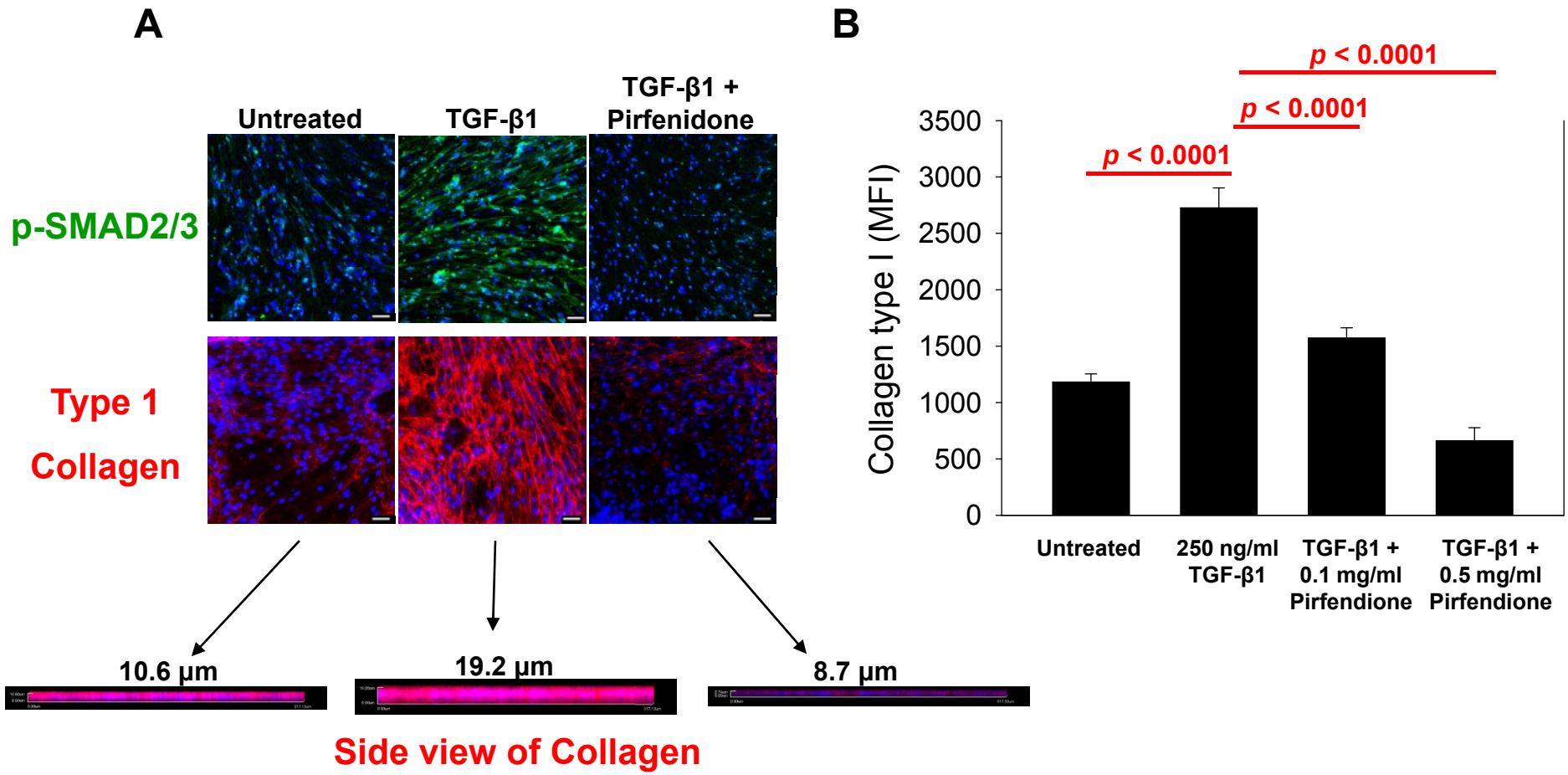

Supplemental Figure 10

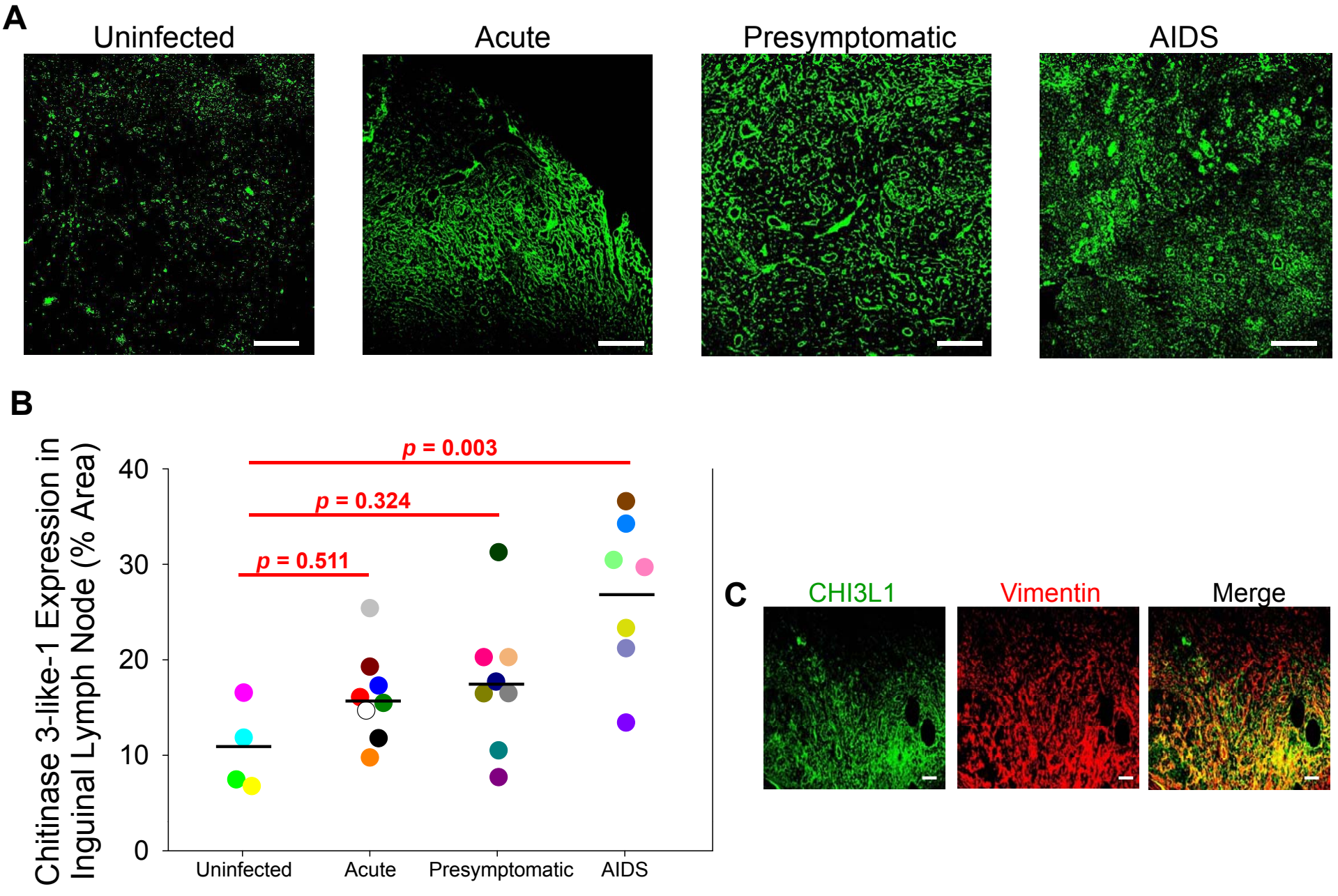

Supplemental Figure 11

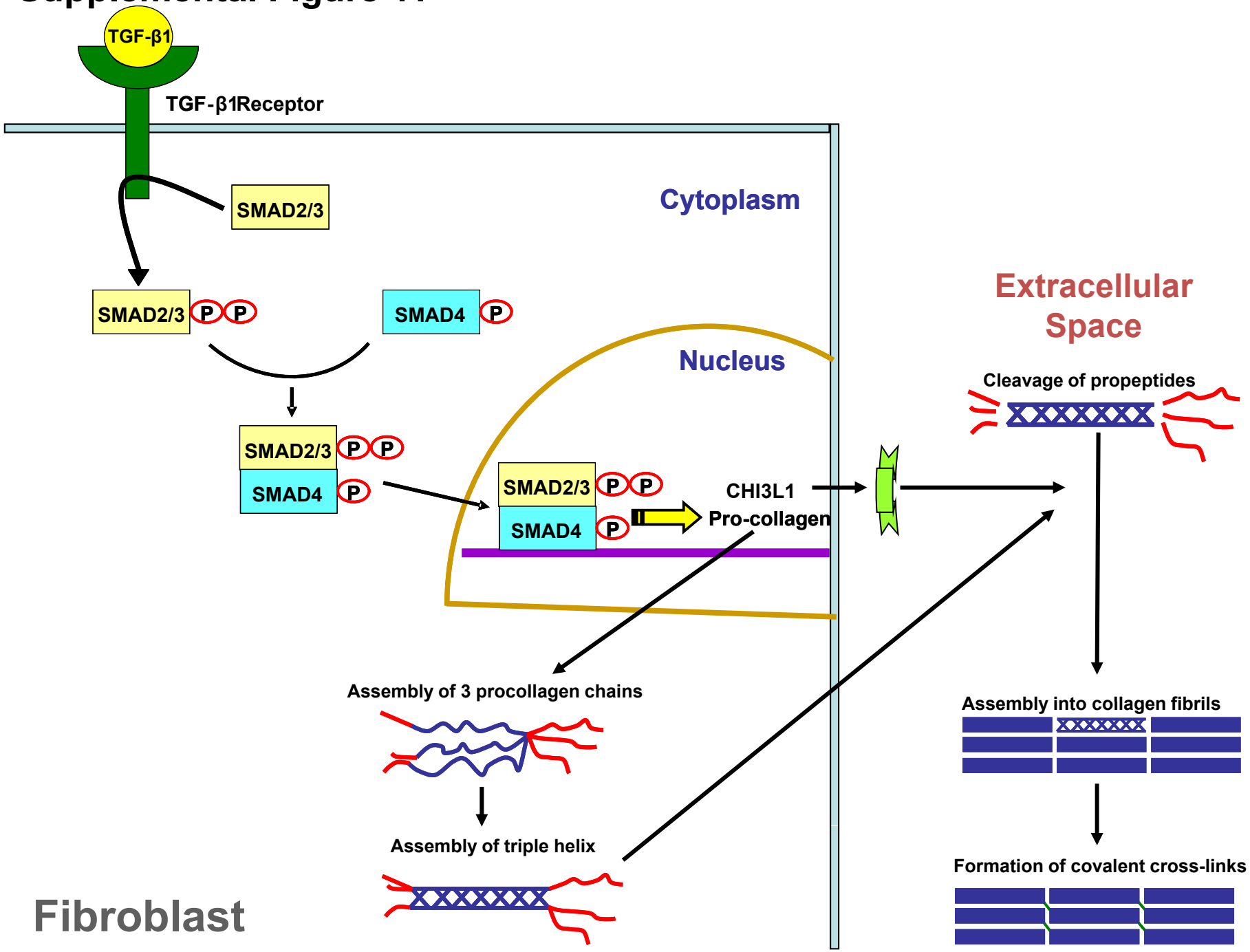

Supplemental Figure 1. Mechanisms of LT fibrosis and damage to the LT niche and depletion of T cells. (**A**) Chronic immune activation in HIV-1 and SIV infections is thought to deplete T cells through increased activation-induced cell death, but immune activation also elicits a T regulatory response that activates TGF-β1 signaling in fibroblasts resulting in cumulative collagen deposition. Collagen deposition impedes access of T cells to the survival factor IL-7 on the FRC network to cause increased apoptosis, which, along with activation-induced cell death, depletes T cells. Depletion of T cells decreases LTβ, which, along with collagen-impeded access to LTβ for FRCs, results in loss of FRC network and IL-7. This vicious cycle of survival interdependencies and collagen deposition cause progressive T cell depletion, particularly in the naïve T cell populations. (**B**) HAART can suppress the loss of CD4+ T cells due to the direct effects of infection and normalize immune activation to reduce losses of CD4+ T cells due to activation-induced cell death. However, pre-existing collagen, loss of FRC

network and T cell depletion will limit immune reconstitution by the continued cyclical mechanisms shown in (**A**).

Supplemental Figure 2. FRCs and FDCs are the major sources of IL-7 in LTs. (**A**) Quantitative image analysis of the percentage of the IL-7 mRNA signal that co-localizes with desmin+ FRCs in T cell zone and FDCs in the B cell follicles. Values are the mean of the percentage of the IL-7 mRNA signal that co-localizes with desmin+ cells ± s.d. (**B**) Confocal image of LN sections from uninfected RMs (representative image for one animal of 3) double immunofluorescently stained for IL-7 (green) and CD1a, CD11c or CD68 (red), showing a small portion of IL-7 is produced by a subset of dendritic cells or macrophages. Scale bar, 30 μm.

Supplemental Figure 3. T cells lose contact with FRCs during SIV infection. (**A-B**) Optical 3D slice showing green stained FRC network and red-stained CD3 T cells in (**A**) an uninfected RM (representative image for one animal of 3) and(**B**) a SIV-infected RM at 180 dpi (representative image for one animal of 4). In the infected animal, much of the FRC network has been lost and T cells are not in contact with FRCs. Scale bar, 20 μm per divide.

Supplemental Figure 4. Loss of FRCs is associated with decreased IL-7 and depletion of naïve T cells within LNs in SIV infection. (**A-B**) Immunohistochemical staining of (**A**) IL-7 and (**B**) desmin in LNs from RMs at different time points post infection. Red arrow points to residual IL-7 and residual FRCs at the B-T cell zone border (representative image for one of 4 animals at each time point). Scale bar, 40 μm. (**C**) Montage image of confocal images of LN section from RMs at 294 dpi stained for CD45RA (red) and CD3 (blue) showing that the residual naïve T cells reside at the B-T border. Scale bar in the inset, 20 μm. (**D-E**) Confocal image of LN sections from uninfected RMs (representative image for one of 4 animals) and RM at 294 dpi stained for CD45RA (green) and CD4 or CD8 (red), showing the progressive and parallel loss of naïve CD4+ and CD8+ T cells within LTs during SIV infection. Scale bar, 30 μm. (**F**)

Quantification of the number of total CD4+ and CD8+ T cells and CD45RA+ naïve CD4+ and CD8+ T cells before and in the chronic phase of infection. Note the rate of the loss of naïve CD8+ T cells is parallel to the loss of naïve CD4+ T cells. (Two-tailed *t* test, n=5, values are the mean of the number of cells ± s.d.)**.**

Supplemental Figure 5. LTβR-Ig treatment and T cell depletion leads to FRC depletion in mouse LNs. (**A-C**) ER-TR-7 staining in LN sections from mice (representative image for one animal of 3) treated with two weekly injections of control IgG (**A**), two weekly injections of LTβR-Ig (**B**), or with 8 weekly injections of CD3 depleting antibody (**C**). Scale bar, 300 μm. (**D-F**) Magnified images of (**A-C**) respectively. Scale bar, 30 μm. (**G**) Quantification of percent area of FRCs in control, LTβR-Ig treated or CD3 depleting antibody-treated mice. Data are expressed as the mean ± s.d..

Supplemental Figure 6. Fibroblasts are the major producers of type I collagen within LT during HIV-1 infection. (**A**) Immunofluorescent images of pro-collagen (red staining) and vimentin (green staining) in the LT from an HIV-1 infected individual in the presymptomatic stage of disease, showing co-localization between pro-collagen and vimentin+ fibroblasts (representative image for one of 4 subjects). Scale bars: 50 μm. (**B**) Immunohistochemical images of vimentin staining (brown) combined with ISH of type I collagen mRNA (yellow/green appearing silver grains due to epipolarized reflected light). Red arrows indicate co-localization between vimentin+ fibroblasts and collagen type I mRNA (representative image for one of 4 subjects in presymptomatic stage). Sense probe shows the negative control staining. Scale bars: 20 μm. (**C**) Immunofluorescent images of vimentin (green staining) and type I collagen (red staining) in primary human fibroblasts isolated from tonsillar tissue from an uninfected individual, revealing basal levels of extracellular type I collagen from an ex vivo culture system 2 days post isolation. Cell nuclei appear blue (DAPI). Scale bars: 30 μm.

Supplemental Figure 7. TGF-β1 expression occurs predominantly in CD3+ T cells while components of the TGF-β1 signaling pathway (TGF-β1 RII, p-SMAD2/3) are expressed in vimentin+ fibroblasts. Immunofluorescent images of (**A**)TGF-β1 (green staining) and CD3 (red staining), (**B**) TGF-β1 RII (red staining) and vimentin (blue staining), (**C**) p-SMAD 2/3 (red staining) and vimentin (green staining) and (**D**) TGF-β1 (green staining) and vimentin (blue staining) in LT from HIV-1 infected individuals (representative image for one of 4 subjects), showing the close spatial proximity between TGF-β1-expressing $CD3^+$ T cells and vimentin+ fibroblasts expressing the TGF-β1 RII. Scale bars: 20 μm.

Supplemental Figure 8. TGF-β1 is mainly produced by CD4+ / Foxp3+ T regulatory cells. (**A**) Immunofluorescent images of TGF-β1 (green staining) and CD4 (red staining), (**B**) TGF-β1 (green staining) and CD8 (red staining), (**C**) TGF-β1 (green staining) and Foxp3 (red staining) in LTs from HIV-1 infected individuals (representative image for one of 4 subjects), showing TGF-β1 expression primarily in CD4+ Foxp3+ T regulatory cells. Scale bars: 20 μm.

Supplemental Figure 9. TGF-β1 stimulates the production of type I collagen by LT fibroblasts. (**A**) Immunofluorescent images of p-SMAD2/3 (green staining) and collagen type I (red staining) in primary human fibroblasts treated with or without TGF-β1 (250 ng/ml) for 48 hr. Addition of the anti-fibrotic drug, pirfenidone (0.1 or 0.5 mg/ml), inhibits the TGF-β1 signaling pathway and decreases collagen type I production (representative image of 10 images). Cell nuclei appear blue (DAPI). Side views of individual collagen type I fibers were captured to display the relative thickness of the extracellular collagen networks in primary LT fibroblasts. Scale bars: 50 μm. (**B**) The extracellular collagen type I networks of primary human fibroblasts were quantified for each condition and reported as collagen type I Mean Fluorescence Intensity (MFI). Data are expressed as the mean ± s.d., where 3 independent experiments were performed in quadruplicate. The results are shown with significance where applicable ($p < 0.05$).

Supplemental Figure 10. CHI3L1 progressively increases within LTs during HIV-1 infection. (**A**) Immunofluorescent images reveal progressive increases in CHI3L1 (green staining) within LT during HIV-1 infection (representative image for all the subjects at each stage). Scale bars: 200 μm. (**B**) CHI3L1 expression was quantified in each LN biopsy and reported as percent tissue area positive for CHI3L1. The results are shown with significance where applicable ($p < 0.05$). Mean values for each group are indicated by horizontal black bars. (**C**) Immunofluorescent images of CHI3L1 (green staining) and vimentin (red staining) in the LT from an HIV-1 infected individual in the presymptomatic stage of disease (representative image for one of 4 subjects), showing co-localization between CHI3L1 and vimentin+ fibroblasts. Scale bars: 50 μm.

Supplemental Figure 11. A model of fibrosis within LT during HIV-1 infection. Increases in TGF-β1-expressing T regulatory cells and its cognate receptor in fibroblasts result in amplification of the TGF-β1 signaling pathway. This leads to increased production of pro-collagen and CHI3L1, a protein which can enhance the maturation of pro-collagen into collagen fibrils. Collectively, these changes accelerate the pathological process of fibrosis.

Supplemental Tables

Supplemental Table 1 Demographic characteristics and clinical information of subjects

Patient	Disease Stage	Gender	Age	Race	Peripheral Blood $CD4^+$ T Cell Count (Cells/μl)	Plasma HIV-1 RNA Levels (Copies/ml)
1425	Uninfected	Male	43	Caucasian	1,351	Undetectable
1442	Uninfected	Female	45	Caucasian	485	Undetectable
1476	Uninfected	Female	28	Caucasian	704	Undetectable
1472	Uninfected	Female	52	Caucasian	837	Undetectable
1455	Acute	Male	23	African American	209	19,400
1391	Acute	Male	37	African American	234	24,718
1389	Acute	Male	32	Caucasian	824	32,173
1449	Acute	Male	30	Caucasian	333	> 100,000
1484	Acute	Male	49	Caucasian	301	23,721
1469	Acute	Male	44	Caucasian	201	>100,000
1458	Acute	Male	51	Caucasian	400	439,000
1435	Acute	Male	42	Caucasian	410	> 100,000
1086	Asymptomatic	Male	30	Caucasian	512	20,562
1293	Asymptomatic	Male	36	Caucasian	905	14,225
1419	Asymptomatic	Male	37	Caucasian	245	61,432
1428	Asymptomatic	Male	30	Caucasian	363	38,600
1436	Asymptomatic	Male	63	Caucasian	248	46,400
1459	Asymptomatic	Male	36	Caucasian	286	> 100,000

1317	Asymptomatic	Male	31	Caucasian	399	120,469
1479	Asymptomatic	Male	42	Caucasian	273	1,650
1413	AIDS	Male	50	African American	42	59,401
1438	AIDS	Male	49	Caucasian	147	4,960
1462	AIDS	Male	43	Caucasian	81	35,000
1327	AIDS	Female	40	African American	112	12,046
1446	AIDS	Female	45	Caucasian	200	150,500
1474	AIDS	Male	40	African American	98	10,000
1263	AIDS	Male	44	Caucasian	3	> 100,000

Supplemental Table 2 List of primary antibodies and antigen retrieval methodologies

Antibody	**Clone/ Manufacturer & Catalog #**	**Antigen-retrieval Pretreatment**	**Antibody Dilution**	**Species**
Desmin	D33 / Lab Vision & # MS-376-S1	Diva Decloaker; High pressure cooker for 30 seconds at 125°C.	1/200	Mouse
Desmin	Polyclonal / Lab Vision & # RB-9014-P1	Diva Decloaker; High pressure cooker for 30 seconds at 125°C.	1/200	Rabbit
CD35	Ber-MAC-DRC / Dako & # M0846	Diva Decloaker; High pressure cooker for 30 seconds at 125°C.	1/100	Mouse

CD21	1F8 / Dako / # M0784	Diva Decloaker; High pressure cooker for 30 seconds at 125°C.	1/100	Mouse
ER-TR7	ER-TR7 / Acris Antibodies & # BM4018	Frozen tissue, Diva Decloaker; Water bath for 5 min at 95°C.	1/200	Rat
CD3	MCA147 / AbD Serotec & # MCA1477	Diva Decloaker; High pressure cooker for 30 seconds at 125°C.	1/200	Rat
CD3	SP7 / Thermo Scientific & # RM-9107-S1	Diva Decloaker; High pressure cooker for 30 seconds at 125°C.	1/100	Rabbit
IL-7	7417 / R & D Systems & # MAB207	Diva Decloaker; High pressure cooker for 30 seconds at 125°C. Proteinase K treatment for 15 min	1/100	Mouse
CD45RA	4KB5 / Dako & # M0754	Diva Decloaker; High pressure cooker for 30 seconds at 125°C.	1/100	Mouse
Activated Caspase-3	8G10 / Cell Signaling Tech. & # 9665	1mm EDTA (ph 8); High pressure cooker for 30 seconds at 125°C.	1/100	Rabbit
Collagen 1	COL-1 / Sigma & # C2456	Diva Decloaker; High pressure cooker for 30 seconds at 125°C. Protease K (10 µg/ml).	1/100	Mouse
Lymphotoxin-β	135105 / R & D Systems &	Diva Decloaker; High pressure cooker for 30 seconds at 125°C.	1/100	Mouse

	# MAB1684			
CD4	Polyclonal / R & D Systems & # AF-379-NA	Diva Decloaker; High pressure cooker for 30 seconds at 125°C.	1/100	Goat
CD4	1F6 / Novacastra & # NCL-CD4–1F6	Diva Decloaker; High pressure cooker for 30 seconds at 125°C.	1/100	Mouse
CD8	SP16 / Neomarkers & # RM-9116-s	Diva Decloaker; High pressure cooker for 30 seconds at 125°C.	1/100	Rabbit
Lymphotoxin-β	Polyclonal / Santa Cruz Biotech. & # sc-23561	Diva Decloaker; High pressure cooker for 30 seconds at 125°C.	1/100	Goat
Vimentin	Vim 3B4 / DAKO & # M7020	Diva Decloaker; High pressure cooker for 30 seconds at 125°C.	1/100	Mouse
Vimentin	Polyclonal / Neomarkers & # Rb-9063-P1	Diva Decloaker; High pressure cooker for 30 seconds at 125°C.	1/100	Rabbit
TGF-β1	Polyclonal / Santa Cruz & # SC-146-G	Diva Decloaker; High pressure cooker for 30 seconds at 125°C. Protease K (10 µg/ml).	1/100	Goat
Collagen I	Polyclonal / Abcam & # ab292	Diva Decloaker; High pressure cooker for 30 seconds at 125°C. Protease K (10 µg/ml).	1/200	Rabbit
Pro-collagen	M-58 /	Diva Decloaker; High pressure cooker for 30 seconds at 125°C.	1/50	Rat

	Millipore & # MAB1912	Protease K (10 µg/ml).		
TGF-β RII	Polyclonal / R & D Systems & # AF-241-NA	Diva Decloaker; High pressure cooker for 30 seconds at 125°C. Protease K (10 µg/ml).	1/100	Goat
Ki-67	SP6 / Neomarkers & # RM-9106-S1	Diva Decloaker; High pressure cooker for 30 seconds at 125°C.	1/200	Rabbit
p-SMAD2/3	Polyclonal / Santa Cruz & # SC-11769	Diva Decloaker; High pressure cooker for 30 seconds at 125°C. Protease K (10 µg/ml).	1/50	Goat
CHI3L1	Polyclonal / Quidel & # 4815	Diva Decloaker; High pressure cooker for 30 seconds at 125°C. Protease K (10 µg/ml).	1/200	Rabbit
IgG Isotype Controls	Dako, Jackson ImmunoResearch	Diva Decloaker; High pressure cooker for 30 seconds at 125°C. Protease K (10 µg/ml).	1/50-1/200	Mouse, Rabbit, Rat, Goat